When Orifice Flow Must Consider Extensional Effects

Austin Zapata

Andrea Vacca

Purdue University, zapata1@purdue.edu

Abstract.

Orifice flows are a fundamental building block of hydraulic pumps and systems, but the complex physics within them is often simplified in frequently-used relationships for ease-of-use. When polymer melts which exhibit strong non-Newtonian behaviors are used, though, these phenomena become dominant and have significant effects on the flow behavior, leading to inaccuracies if the orifice equation is used. Typical orifice relationships often consider only the effect of flow regime, which is captured by the Reynolds number. The ratio of extensional to shearing flow, often called the Trouton ratio, must be considered in some specialized cases. This study will develop an orifice model which accounts for extensional effects of the fluid by a relationship between dimensionless parameters: the Euler number, the Reynolds number, and the Trouton ratio. The use cases of this expression are then detailed. The model is developed using experimental data of pressure drop and flow for six different fluids across which there are a total of 282 data points. The model's coefficient of correlation is shown to be 0.9990, demonstrating the high accuracy of this model across a wide range of Reynolds numbers.

Keywords. Orifice flow, orifice equation, complex fluids, viscosity.

1. INTRODUCTION

Orifice flows frequently appear in the analysis of hydraulic systems and components. These flows are characterized by their strong dependence on a variety of fluid properties and flow characteristics. In fluid power applications, these flows influence the pressurization of volumes within pumps and systems, such as displacement chambers, hydraulic cylinder chambers, and the flow through valves. It is crucial, then, to have a known relationship between the flow and pressure drop for an orifice. In academia and industry, it is nearly ubiquitous to utilize the orifice equation for these flows, shown below, which is derived from the Bernoulli's equation and conservation of energy.

$$Q = C_d A \sqrt{\frac{\Delta p}{\rho}} \tag{1.1}$$

The orifice equation is often used to model the internal flows of positive displacement machines [1, 2, 3, 4] where constricted flow between volumes is often characterized as orifice flow. The discharge coefficient, given by C_d in Eq. (1.1), accounts for losses in the orifice due to contraction, vortex development, friction, and other factors.

The problem faced by this study, though, cannot be accurately described by Eq. (1.1). The fluids being studied follow the Williamson model [5], which is a viscosity function characterized by a Newtonian plateau at low shear rates and a power law region at high shear rates. These polymer melts also exhibit other non-Newtonian behavior in their elasticity, which greatly effects flow in turbulent conditions and at the entrance of an orifice.

The fundamental work of Smith et. al. [6] was one of the first to parameterize this coefficient. Over the proceeding century, a vast quantity of work has been performed to determine the effect of the orifice diameter ratio on the boundary layer and vortex development in the orifice [7, 8], quantifying how laminar flow leads to lower discharge coefficients [9], what parameters affect regime change in orifice flow [10], and the effect of flow disturbances caused by cavitation on frictional loss [11, 12]. All of the work previously mentioned, though, assumed the flow of a Newtonian fluid, but in this case non-Newtonian operating fluids are used and thus these correlations are not applicable.

Previous approaches to modeling non-Newtonian orifice flow have been quite similar to those for Newtonian fluids. Some of these works, such as those by Dziubiński et. al. [13] and Ntamba et. al. [14], capture non-Newtonian effects by altering the discharge coefficient within the orifice equation. Others, such as Bohra et. al. [15] and Rituraj et. al. [16] form relationships between dimensionless parameters based on experimental results to determine the flow. These are the orifice diameter ratio β, which is the ratio of the orifice diameter to the surrounding pipe diameter, and the aspect ratio, which is defined as the ratio of the orifice length to its diameter.

Relevant to this study are the flows within hydraulic pumps and motors, which are characterized by small values of β and aspect ratios approaching zero, meaning the orifices are sharp. This is because the pressurization of displacement chambers typically occurs when small connections exist between the displacement chambers and the ports. Both of these geometrical considerations must be modeled correctly to maintain the accuracy of flow predictions. The only study which studied flows with non-Newtonian fluids through sharp orifices with small diameter ratios, though, was that from Rituraj et. al. [16]

All of these studies, though, neglect the effect of extensional behavior on the flow. Extension rates are the diagonal components of the extra-stress tensor, and they greatly influence boundary layer formation and vortex development at the entrance of the orifice as discussed in [17]. A simple example of extension is seen below in Figure 1.1, which shows the fluid velocity profile at the entrance of a pipe.

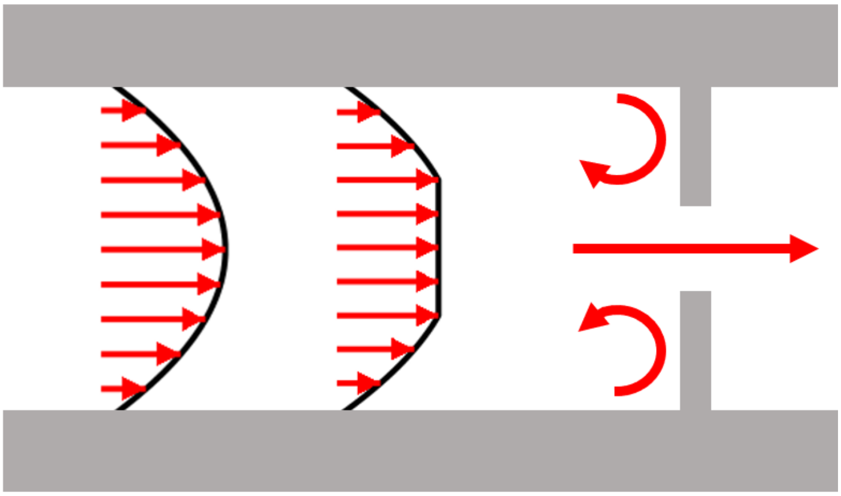

Figure 1.1. Fluid velocity at pipe entrance

As seen in the figure, the fluid flow leading up to the orifice entrance is parabolic as expected in laminar flow. As the fluid approaches the orifice, though, the profile takes on a straighter shape and eventually breaks down as vortices form at the corners between the orifice and the walls, and the resulting streamline through the orifice has a higher velocity than the initial pipe flow. A flow profile like Figure 1.1 is shown in [18]. A consequence of this is that the fluid velocity in the x direction, as denoted in the figure, is changing along the x direction. This is defined as an extension, of the fluid, shown in its mathematical form in Eq. (1.1), below. In this case, the extension would be negative, which is also classified as a contraction of the fluid.

$$\dot{\boldsymbol{\epsilon}} = \begin{bmatrix} \frac{\partial u_x}{\partial x} & \frac{\partial u_y}{\partial y} & \frac{\partial u_z}{\partial z} \end{bmatrix}^T \tag{2.4}$$

It is apparent from Figure 1.1 that this geometric strongly resembles that of an orifice, and thus extensional effects may heavily influence the loss across the orifice. Existing literature on orifice models, though, often neglects these effects. Jones et. al. [19] demonstrated how two distinct fluids with the same shear-viscosity, in this case a Newtonian fluid and a Boger fluid, can have distinct extensional characteristics, and this is a factor which current orifice models for non-Newtonian fluids neglect. Papaevangelou [20] found that the Trouton ratio [21], which is the ratio of extensional-to-shear viscosity, can be upwards of 70 in orifice flow of shear-thinning fluids, whereas the Trouton ratio for a Newtonian fluid is always three. Ascanio et. al. [22] found a correlation between the Euler number, Reynolds number, and Trouton ratio for flow through a conical die. All fluids they tested exhibited significant shear-thinning behavior, but their elastic properties were quite distinct which led to differing relationships between pressure and flow for each fluid tested.

The state-of-the-art demonstrates the significance of elastic and extensional effects in the orifice flow of non-Newtonian fluids, but there is no existing literature for sharp orifices with small orifice diameter ratios for non-Newtonian fluids which considers these extensional effects. This study aims to derive and verify an orifice expression for Williamson fluids in sharp orifices with small orifice diameter ratios which can capture the elasticity of the fluid by incorporating the Trouton ratio. This expression will be limited to applications using Williamson fluids, but its general form can be utilized for other polymer melts, such as the Carreau-Yasuda fluids from [16], by training similar experimental data from those fluids to find the constants.

With the objectives of the study laid out, the organization of this paper is now detailed. In Section 2, a closed-form expression for the Trouton ratio is developed in terms of measurable parameters and a corresponding orifice relationship is proposed. In Section 3, the experimental setup is discussed including the fluids which are tested and the components used. In Section 4, experimental results are shown and used to identify the unknowns from the model proposed in Section 2, thereby completing the study. Finally, conclusions are drawn based on these results.

2. METHODOLOGY

Two primary methods commonplace in the creation of an orifice model are, as discussed in the introduction, fitting an expression to the discharge coefficient or by fitting a relationship between dimensionless parameters. For this study, the latter method has been selected due to the prior research done on sharp orifices with non-Newtonian fluids. The prior work done on these flows, such as that by Rituraj and Vacca [16], demonstrates the advantages of relating dimensionless parameters via the Buckingham π theorem. Their existing model, shown in Eq. (2.1), considers four dimensionless parameters: the Euler number Eu, which captures energy losses in the flow, the Reynolds number Re, which quantifies the flow regime, the orifice diameter ratio β, which affects vortex and boundary layer development, and the Weissenberg number Wi, which captures the viscoelasticity of the fluid.

$$\mathrm{Eu} = \frac{k_1}{\mathrm{Re}^{k_2}} \beta^{k_3} \mathrm{Wi}^{k_4} \tag{2.1}$$

$$\mathrm{Eu} = \frac{\Delta p}{\frac{1}{2}\rho v^2} \tag{2.2}$$

$$\mathrm{Re} = \frac{\rho v d}{\eta} \tag{2.3}$$

$$\beta = \frac{d}{D} \tag{2.4}$$

$$\mathrm{Wi} = \lambda \dot{\gamma} \tag{2.5}$$

To consider extensional effects, though, the model must use an additional parameter. This parameter which quantifies the effect of extension rate in the flow is the Trouton ratio [21], defined by Eq. (2.6).

$$\mathrm{Tr} = \frac{\eta_{Ex}}{\eta} \tag{2.6}$$

Cogswell [23] proposed a model, later dubbed the Cogswell model, for purely-extensional polymer flow which parameterized the extension rate, extensional stress, and extensional viscosity in a capillary rheometer as shown in Eq. (2.7-2.9) respectively below. Because the capillary rheometer has a similar geometry to an orifice, with a flow constriction between two pipes, the authors assume these expressions correlate well to orifice flows.

$$\dot{\epsilon} = \frac{4}{3(n+1)}\frac{\eta\dot{\gamma}}{\eta_{Entrance}} \tag{2.7}$$

$$\sigma_E = \frac{3(n+1)}{8}\eta_{Entrance}\dot{\gamma} \tag{2.8}$$

$$\eta_{Ex} = \frac{\sigma_E}{\dot{\epsilon}} \tag{2.9}$$

Where n is the power law index of the fluid, $\eta_{Entrance}$ is the shear viscosity at the capillary entrance, $\dot{\gamma}$ is the apparent shear rate, and η is the shear viscosity at the end of the rheometer. An unknown here is the shear viscosity at the capillary entrance, which is difficult to obtain experimentally, but Ye et. al. [24] offered a correlation given by Eq. (2.10).

$$\eta_{Entrance} = \frac{\Delta p}{\dot{\gamma}} \tag{2.10}$$

Substitution of Eq. (2.7-9) into Eq. (2.6) yields the expression for the Trouton ratio, shown in Eq. (2.11)

$$\mathrm{Tr} = \frac{9}{32}\left((n+1)\frac{\Delta p}{\eta\dot{\gamma}}\right)^2 \tag{2.11}$$

The shear rate in this equation is given by Eq. (2.12), which was initially derived by Metzner and Reed [25] and later used by Dziubinski et. al. [13] and Rituraj et. al. [16] in works related to non-Newtonian orifice modeling.

$$\dot{\gamma} = \frac{3n+1}{4n}\frac{32Q}{\pi d^3} \tag{2.12}$$

The shear viscosity, naturally, is also a function of the shear rate. Now that the Trouton ratio has been expressed in terms of fluid parameters and flow properties, an orifice expression can be derived of the form in Eq. (2.13).

$$\mathrm{Eu} = \frac{k_1}{\mathrm{Re}^{k_2}}\beta^{k_3}\mathrm{Wi}^{k_4}\mathrm{Tr}^{k_5} \tag{2.13}$$

This expression takes the same form as that in the state-of-the-art [16], but has been adjusted to include the Trouton ratio, which will account for the extensional effects of the working fluids. This expression does, though contain five different constants which must be determined. This is achieved through a set of experiments varying pressure, orifice diameter, and fluid as discussed in the next section.

3. EXPERIMENTAL SETUP

The hydraulic circuit for the experimental setup used to obtain the fluid data is given in Figure 3.1. An electric motor drives an external gear machine, which for this study was a MAAG CHEM 25 unit, which then delivers this flow through an orifice. Three orifice diameters were tested, which resulted in orifice diameter ratios of 0.16, 0.08, and 0.04. The hydraulic line leading to the orifice has a diameter of 29 mm. Two pressure transducers, P1 and P2, were placed upstream and downstream, respectively, of the orifice to measure the pressure drop. The flow rate is then measured via a Coriolis type flow meter. A pressure relief valve is placed after the flow meter to allow control over the pressure downstream from the orifice.

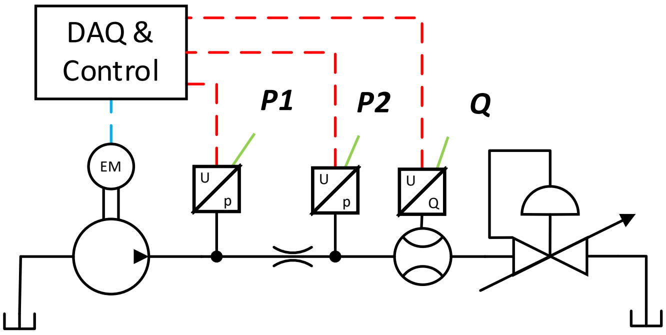

Figure 3.1. ISO Schematic of the Experimental Hydraulic Circuit

For the fluids in question, the viscosity-shear rate relationship follows the Williamson model [5], shown by Eq. (3.1). This relationship is characterized by a Newtonian plateau at low shear rates, where the viscosity is close to η_0, dubbed the zero-shear rate viscosity, and a power law region at high shear rates, the slope of which is determined by the power law index n. The transition between these two regions is controlled via the characteristic time λ.

$$\eta = \frac{\eta_0}{1 + (\lambda\dot{\gamma})^{1-n}} \tag{3.1}$$

Three distinct shear-thinning fluids were tested for this study, all of which closely adhere to the Williamson model, as shown via Figure 3.2. These fluids have zero shear rate viscosities ranging from 5 - 100 $Pa \cdot s$, power law indices between 0.4 - 0.6, and characteristic times between 0.001 - 0.1 s. Further information on these fluids cannot be disclosed due to confidentiality.

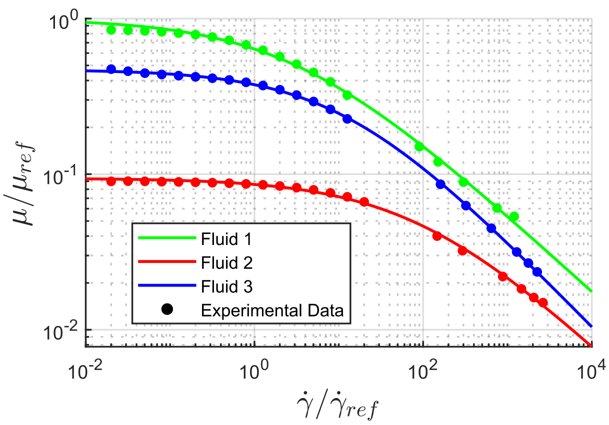

Figure 3.2. ISO Schematic of the Experimental Hydraulic Circuit

Experiments are conducted over a wide range of conditions by varying the pump speed, orifice diameter, and back pressure P2. At each data point, the pressure on both sides of the orifice and flow are recorded. Overall, 282 data points were collected with which the model was trained.

4. Model Development

The experimental data for pressure, flow, and fluid properties was used to obtain the dimensionless parameters in Eq. (2.13) at each data point. This data is collected in Figure 4.1 below. The trend of Re versus Eu aligns with expectations [16], that being a negative linear relationship on a log-log scale. Variation from this line is in large-part due to the factors discussed in Section 2, those being the vortex and boundary layer development, fluid viscoelasticity, and extensional effects of the fluid.

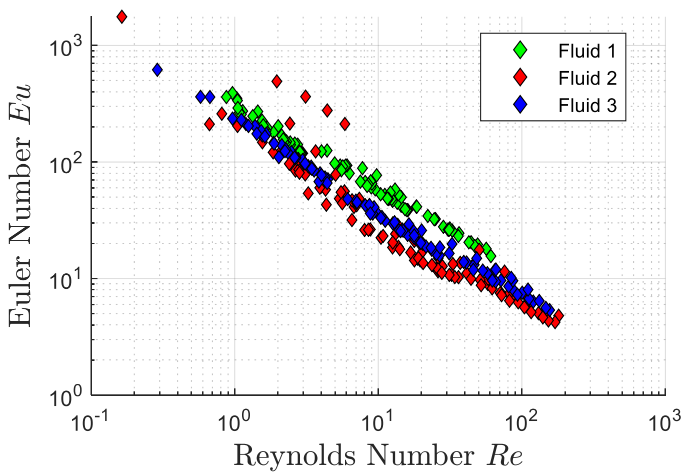

Figure 4.1. Experimental Data of all three fluids for the Reynolds number versus Euler number

The correlation proposed by Eq. (2.13) is then trained to determine the values of the constants k_1, k_2, k_3, k_4 and k_5 via a least-squares multiple linear regression analysis performed on a logarithmic scale to minimize errors across the data collected, which spanned multiple orders of magnitude, and to adhere to the linear trend observed in Figure 4.1 on a log-log- scale. The constants obtained for this analysis are shown in Table 4.1.

Constant	Value
$\boldsymbol{k_1}$	30.1402
$\boldsymbol{k_2}$	0.9865
$\boldsymbol{k_3}$	0.0116
$\boldsymbol{k_4}$	0.0059

$\boldsymbol{k_5}$	0.4684

Table 4.1. Constants for the proposed relationship

This makes the final correlation:

$$\mathrm{Eu} = \frac{30.1402}{\mathrm{Re}^{0.9865}} \beta^{0.0116} \mathrm{Wi}^{0.0059} \mathrm{Tr}^{0.4684} \tag{4.1}$$

The coefficient of correlation for this relationship is $R^2 = 0.9990$. The range of applicability for this correlation is $0.1 < Re < 200$ and $0.04 \leq \beta \leq 0.16$. Figure 4.2 shows the experiments and predictions overlayed separated by fluid, which demonstrates the high correlation between this model and the experimental data.

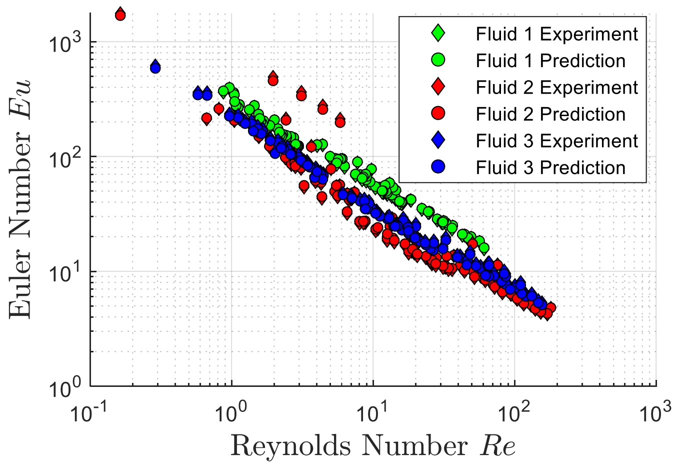

Figure 4.2. Reynolds number versus Euler number for the experiment and the proposed orifice model

Figure 4.3 also serves to validate the model by comparing the measured Euler number versus the predicted Euler number. The plot shows how closely the data points follow the ideal curve, that being the $y = x$ line.

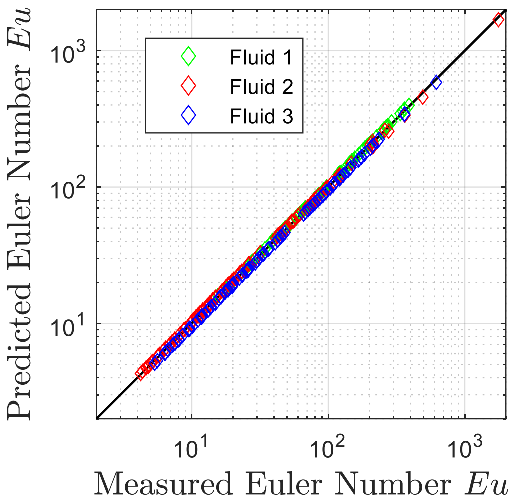

Figure 4.3. Measured versus predicted Euler number for the proposed orifice model

To validate the proposed orifice model, the expression developed is tested on a separate set of experimental data from those points used to train it. The data from Rituraj and Vacca [16] is utilized to test its efficacy to other fluids of similar non-Newtonian characteristics on which the model was not developed. The results of this can be seen in Figure 4.4

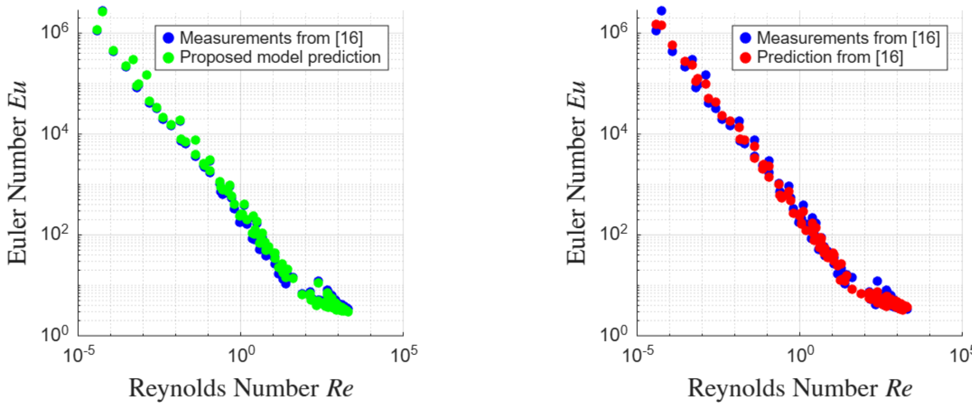

Figure 4.4. Validation results for the proposed orifice model compared to that from [16]

Figure 4.4 visually shows the clear improvement of the consideration of the Trouton ratio on the accuracy of the orifice model, even using data on which the model was not trained. Numerical analysis further supports this claim. While the standard error of the orifice model from [16] is 0.0020, the model proposed by this study has a standard error of 0.0013, showing a marked improvement. This serves to validate both the generalizability of this orifice model and the importance of the consideration of extensional effects on orifice flows for non-Newtonian fluids.

5. CONCLUSION

In this study, an orifice model was proposed for sharp orifice flows with non-Newtonian fluids to consider the extensional behavior of the fluid and its effect on the effective viscosity. An expression for the Trouton ratio was developed in terms of parameters from the Cogswell model. Experiments ranging across orifice diameter ratios of 0.04, 0.08, and 0.16 were tested with pressure differences between 2-50 bar and flows ranging from 0.1-1.5 L/min. The experimental data was then used to develop a model relating the Euler number to the Reynolds number, the orifice diameter ratio, the Weissenberg number, and the Trouton ratio. The derived relationship is applicable to polymer melts which exhibit prominent shear-thinning behavior and obey the Williamson fluid model. The relationship derived successfully parameterizes the flow across the orifice in terms of fluid properties, orifice geometry, and the pressure drop, as shown by its correlation coefficient of 0.9990 with the experimental data. This model was then validated using experimental data from a previous study, showing that the proposed model gives improved predictions from the state-of-the-art for data on which it was not trained.

6. REFERENCES

[1] D. Pan and A. Vacca, "Modeling of Crescent-Type Internal Gear Pumps Considering Gear Radial Micromotion," *Chemical Engineering & Technology,* vol. 46, no. 1, pp. 128-136, 2022.

[2] A. Vacca, S. Dhar and T. Opperwall, "A Coupled Lumped Parameter and CFD Approach for Modeling External Gear Machines," in *The 12th Scandanavian International Conference on Fluid Power*, Tampere, 2011.

[3] A. Vacca and M. Guidetti, "Modelling and experimental validation of external spur gear machines," *Simulation Modelling Practice and Theory,* vol. 19, pp. 2007-2031, 2011.

[4] M. Eaton, P. S. Keogh and K. A. Edge, "The modelling, prediction, and experimental evaluationof gear pump meshing pressures with particularreference to aero-engine fuel pumps," *Proceedings of the Institution of Mechanical Engineers, Part I: Journal of Systems and Control Engineering,* vol. 220, no. 5, pp. 365-379, 2006.

[5] R. V. Williamson, "The Flow of Pseudoplastic Materials," *Industrial & Engineering Chemistry,* vol. 21, no. 11, pp. 1108-1111, 1929.

[6] D. Smith and W. Walker, "Orifice Flow," *Proceedings of the Institution of Mechanical Engineers,* vol. 104, no. 1, pp. 23-36, 1923.

[7] F. Shan, Z. Liu, W. Liu and Y. Tsuji, "Effects of the orifice to pipe diameter ratio on orifice flows," *Chemical Engineering Science,* vol. 152, pp. 497-506, 2016.

[8] B. Gulsacan, N. Tokgoz, E. Karakas, M. Aureli and C. Evrensel, "Effect of orifice thickness-to-diameter ratio on turbulent orifice flow: An experimental and numerical

investigation," *International Communications in Heat and Mass Transfer,* vol. 151, p. 107213, 2024.

[9] W. Borutzky, B. Barnard and J. Thoma, "An orifice flow model for laminar and turbulent conditions," *Simulation Modelling Practice and Theory,* vol. 10, no. 3-4, pp. 141-152, 2002.

[10] Y. Yan and R. B. Thorpe, "Flow regime transitions due to cavitation in the flow through an orifice," *International Journal of Multiphase Flow,* vol. 16, no. 6, pp. 1023-1045, 1990.

[11] K. Sato and Y. Saito, "Unstable Cavitation Behavior in a Circular-Cylindrical Orifice Flow," *JSME International Journal Series B Fluids and Thermal Engineering,* vol. 45, no. 3, pp. 638-645, 2002.

[12] S. Dabiri, A. Sirignano and D. Joseph, "A numerical study on the effects of cavitation on orifice flow," *Physics of Fluids,* vol. 22, no. 4, p. 042102, 2010.

[13] A. Marcinkowski and M. Dziubiński, "Discharge of Newtonian and non-Newtonian Liquids from Tanks," *Chemical Engineering Research and Design,* vol. 84, no. 12, pp. 1194-1198, 2006.

[14] B. N. Ntamba and V. Fester, "Pressure Losses and Limiting Reynolds Numbers for Non-Newtonian Fluids in Short Square-Edged Orifice Plates," *Journal of Fluids Engineering,* vol. 134, no. 9, p. 091204, 2012.

[15] L. K. Bohra, L. Mincks and S. Garimella, "Experimental Investigation of Pressure Drop Characteristics of Viscous Fluid Flow Through Small Diameter Orifices," *Journal of Fluids Engineering,* vol. 143, no. 2, p. 021306, 2021.

[16] R. and A. Vacca, "Modeling the Flow of Non-Newtonian Fluids Through Sharp Orifices," *Journal of Fluids Engineering,* vol. 140, 2018.

[17] M. D. J., "Extensional flow of non-newtonian fluids—A review," *Polymer Engineering and Science,* vol. 11, no. 6, pp. 433-445, 1971.

[18] T. C. H., "A revisitation of generalized newtonian fluids," *Journal of Rheology,* vol. 64, no. 3, pp. 493-504, 2020.

[19] D. M. Jones, K. Walters and P. R. Williams, "On the extensional viscosity of mobile polymer solutions," *Rheologica Acta,* vol. 26, pp. 20-30, 1987.

[20] G. Papaevangelou, "The flow through an orifice of semi-rigid-polymer solutions," in *International Conference on Continuum Mechanics*, Chalkida, Greece, 2006.

[21] F. Trouton, "On the coefficient of viscous traction and its relation to that of Viscosity," *Proceedings of the Royal Society of London. Series A, Containing Papers of a Mathematical and Physical Character,* vol. 77, no. 519, pp. 426-440, 1906.

[22] G. Ascanio, P. Carreau, E. Brito-De La Fuente and P. Tanguy, "Orifice Flowmeter for Measuring ExtensionalRheological Properties," *The Canadian Journal of Chemical Engineering,* vol. 80, pp. 1189-1196, 202.

[23] F. N. Cogswell, Polymer Melt Rheology: A Guide for Industrial Practice, Woodhead Publishing, 1981.

[24] Q. Ye, W. Niemeier, O. Tiedje and B. Shen, "Determining extensional viscosity from the measured pressure drop in a capillary rheometer for paint liquids based on fluid dynamic simulations," *Journal of Non-Newtonian Fluid Mechanics,* vol. 343, p. 105444, 2025.

[25] A. B. Metzner and J. C. Reed, "Flow of non-newtonian fluids—correlation of the laminar, transition, and turbulent-flow regions," *American Institute of Chemical Engineers Journal,* vol. 1, no. 4, pp. 434-440, 1955.